Accepted Manuscript

Synthesis and anticancer activity of new dihydropyrimidinone derivatives

Amany S. Mostafa, Khalid B. Selim

PII: S0223-5234(18)30560-9

DOI: 10.1016/j.ejmech.2018.07.004

Reference: EJMECH 10539

To appear in: *European Journal of Medicinal Chemistry*

Received Date: 16 April 2018

Revised Date: 1 July 2018

Accepted Date: 2 July 2018

Please cite this article as: A.S. Mostafa, K.B. Selim, Synthesis and anticancer activity of new dihydropyrimidinone derivatives, *European Journal of Medicinal Chemistry* (2018), doi: 10.1016/j.ejmech.2018.07.004.

Graphical Abstract

Synthesis and anticancer activity of new dihydropyrimidinone derivatives

Amany S. Mostafa and Khalid B. Selim

A series of dihydropyrimidinone derivatives bearing various heteroaryl moieties was designed, synthesized and evaluated for anticancer activity. Compound **19** possessed the most significant activity against NCI-H460, SK-MEL-5 and HL-60(TB) cell lines. It proved to have dual inhibitory effect against VEGFR-2 and m TOR. Cell cycle analysis of A549 cells showed cell cycle arrest at G2/M phase and pro-apoptotic activity.

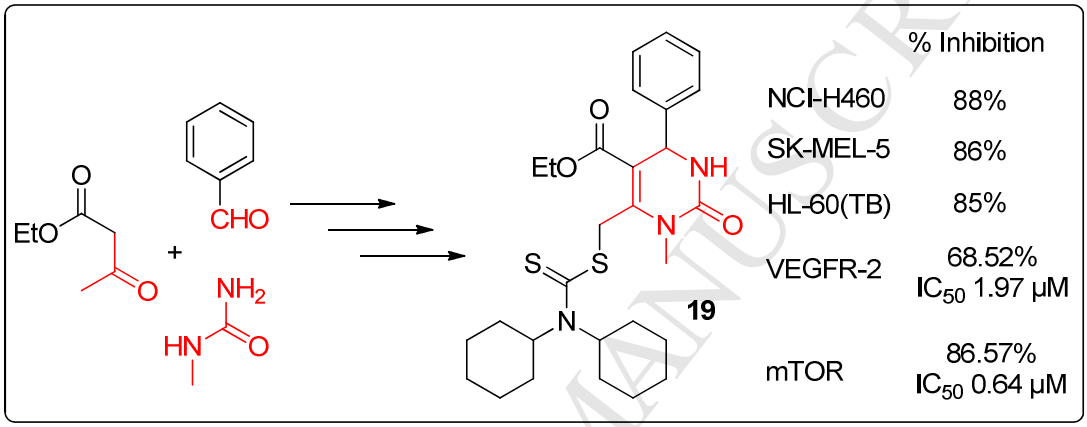

Synthesis and anticancer activity of new dihydropyrimidinone derivatives

Amany S. Mostafa and Khalid B. Selim*

Department of Pharmaceutical Organic Chemistry, Faculty of Pharmacy, Mansoura University, Mansoura 35516, Egypt

*Corresponding author: K. B. Selim
e-mail: khbselim@mans.edu.eg
tel: +2050-2247496 fax: +2050-2247496

Abstract
A series of dihydropyrimidinone derivatives bearing various *N*-heterocyclic moieties was designed and synthesized. Twelve new compounds were screened for their cytotoxic activity using 60 cancer cell lines according to NCI (USA) protocol. Compound **19** showed a significant activity against NCI-H460, SK-MEL-5, and HL-60(TB) cell lines with growth inhibition 88%, 86% and 85%, respectively, and was found to be more safe on normal cells when compared to doxorubicin. Enzyme inhibition assay was performed for compound **19** against mTOR (IC_{50} = 0.64 μM) and VEGFR-2 (IC_{50} = 1.97 μM) to show high potency in comparison to rapamycin (IC_{50} = 0.43 μM) and sorafenib (IC_{50} = 0.3 μM) as references, respectively. Cell cycle analysis of A549 cells treated with **19** showed cell cycle arrest at G2/M phase and pro-apoptotic activity as indicated by annexin V-FITC staining.

Keywords Dihydropyrimidinone; anticancer; mTOR; VEGFR-2; cell cycle analysis; apoptosis

1. Introduction

Tyrosine kinases (TKs) are responsible for the phosphorylation of tyrosine residues in proteins leading to change the function of protein and consequently involve in cell signaling pathways [1]. Mutations can affect some TKs to become constantly active, leading to the outgrowth of cancer [2]. Among these TKs, vascular endothelial growth factor (VEGF) is an important signaling protein engaged in both vasculogenesis and angiogenesis. VEGF exerts its biological effects through binding to specific TK receptors including VEGFR-1 and VEGFR-2 (Figure 1) [3,4]. It also acts as a survival or an anti-apoptotic factor where it induces B-cell lymphoma 2 (Bcl-2) in endothelial cells as well as in breast cancer cells [5,6]. Therefore, some therapeutic approaches using anti-VEGF/VEGFR2 are currently explored to inhibit proliferation and induce apoptosis of malignant cells in hematologic diseases [7].

The mammalian target of rapamycin (mTOR) is a serine/threonine kinase which plays a critical role in phosphatidylinositol 3-kinase (PI3K)/protein kinase B (Akt) signaling pathway, either through direct phosphorylation or inhibition of the protein phosphatase 2 (PP2A) (Figure 1) [8,9]. This pathway is important in regulating various cell functions, including cell growth, proliferation, survival, autophagy, metabolism and cytoskeletal organization in many cancers. In addition, mTOR has profound effects on the regulation of the programmed cell death, known as apoptosis, which has a significant function in various physiological and pathophysiological circumstances [10,11,12]. mTORs are frequently deregulated in diverse human cancers such as lung cancer, breast cancer and glioblastoma. Based on their vital cellular functions, mTORs have emerged as effective anti-cancer drug targets.

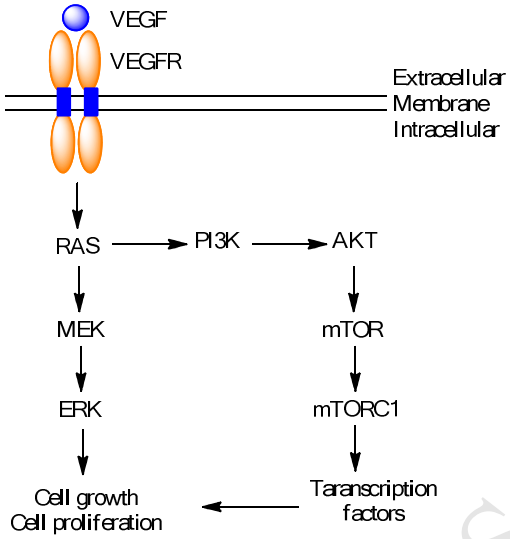

Figure 1. Brief role of VEGF and PI3K/AKT/mTOR pathway in cell growth.

Dihydropyrimidinone (DHPM) derivatives were discovered by Biginelli [13] through multi-component reaction. DHPM is characterized by its multi-functionalized scaffold that exhibits diverse biological activities [14], such as calcium channel blockade, anti-microbial [15], anti-viral [16], anti-oxidant [17,18] and especially anti-cancer activity (Figure 2). These compounds were identified as promising anticancer agents in which monastrol was the most highlighted [19]. Monastrol causes mitotic arrest at G2/M phase by blocking bipolar mitotic spindle in mammalian cells leading to cell apoptosis [20].

Since then, monastrol has inspired the medicinal chemists to design new anticancer agents through molecular manipulation of the DHPM scaffold by modifying the substituents regarding their electronic and lipophilic nature. Extensive substitutions (R_1, R_2, R_3, R_4 and X) were placed on different positions of the ring aiming to obtain potent anticancer agents such as dimethylenastron [21], compounds **1** [22], **2** [23] and **3** [24] (Figure 2). However, modification of substituent R_5 at C6 has not been well exploited, where most of the reports were limited to compounds that show antihypertensive activity other than anticancer activity.

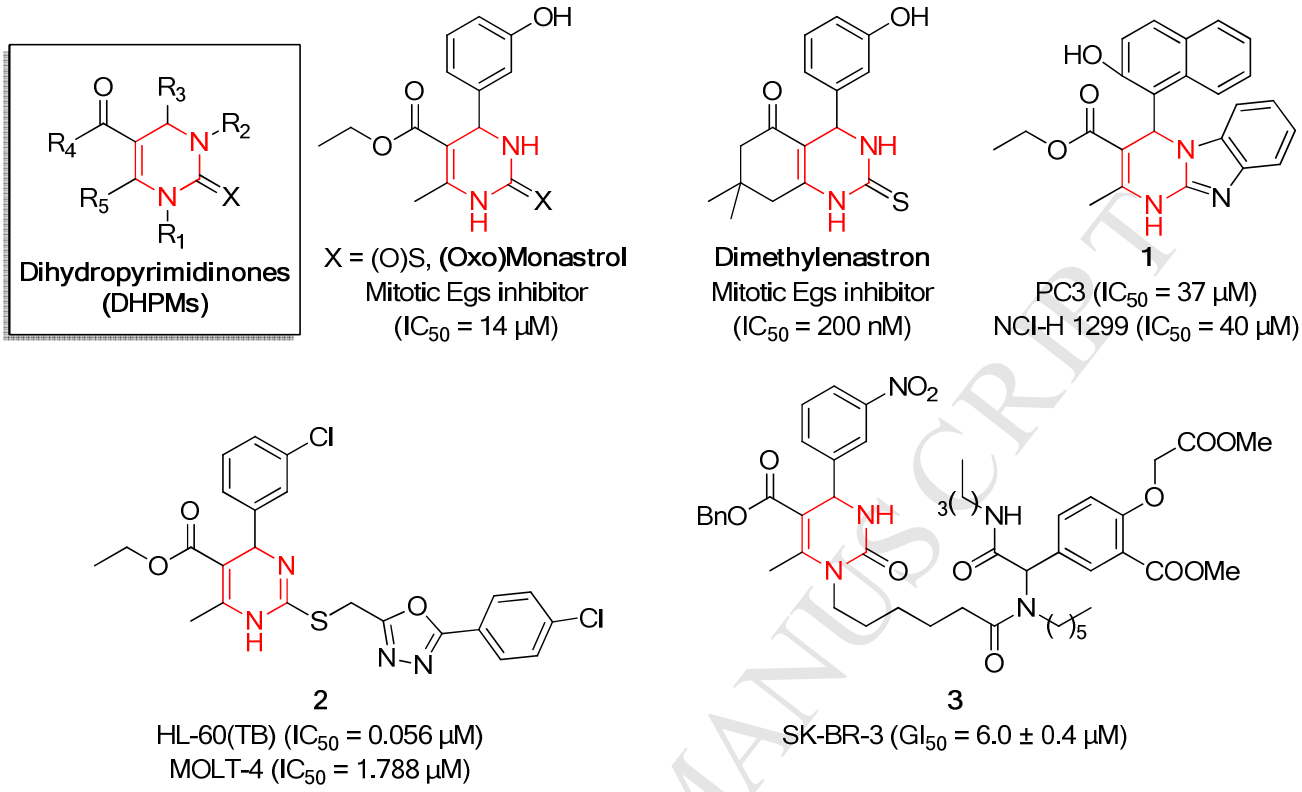

Figure 2. Structures of some DHPM derivatives with anticancer activity.

On the other hand, the azole heterocycles (including thiazoline, tetrazole, 1,3,4-oxadiazole, benzimidazole, 1,2,3-triazole, and cyclic amines) play an important role in improving pharmacokinetic and pharmacodynamic properties of anticancer drugs by enhancing lipophilicity, polarity or the physicochemical properties (Figure 3) [25, 26]. The presence of dithiocarbamate linkage in various natural and synthetic molecules was proved to be crucial to their inhibitory activities against cancer cells [27]. These findings have encouraged us to investigate the potential synergistic effect of the molecular hybridization between DHPM nucleus and azole heterocycles *via* a methyl (thio) or dithiocarbamate bridge at C6 with the aim of exploring the impact of such modification on the anticancer activity.

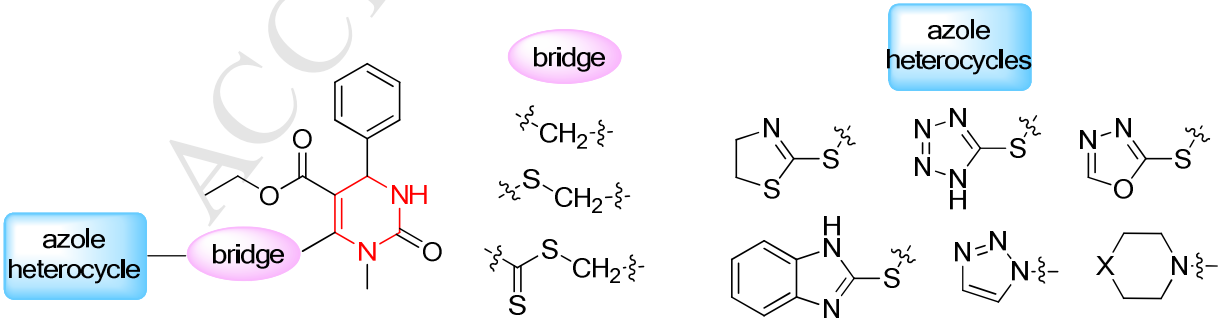

Figure 3. Molecular hybridization of DHPM scaffold with different azole heterocyles at C6.

Taking into consideration the value of DHPM scaffolds, this work aimed to construct novel candidates

of anticancer drugs structurally related to monastrol, using the Biginelli reaction. Twelve of the synthesized compounds were evaluated for their *in vitro* cytotoxicity according to the current single-dose protocol of the National Cancer Institute (NCI) assay against a panel of 60 tumor cell lines. The most potent compounds were further investigated for their activities against human normal cell lines (MCF5, BJ, WPE1-NA22) and for their effect on cell death and cell cycle distribution as well as the enzymatic inhibitory activity on mTOR and VEGFR (as a possible credible mechanism behind their anticancer efficacy).

2. Results and discussion

2.1. Chemistry

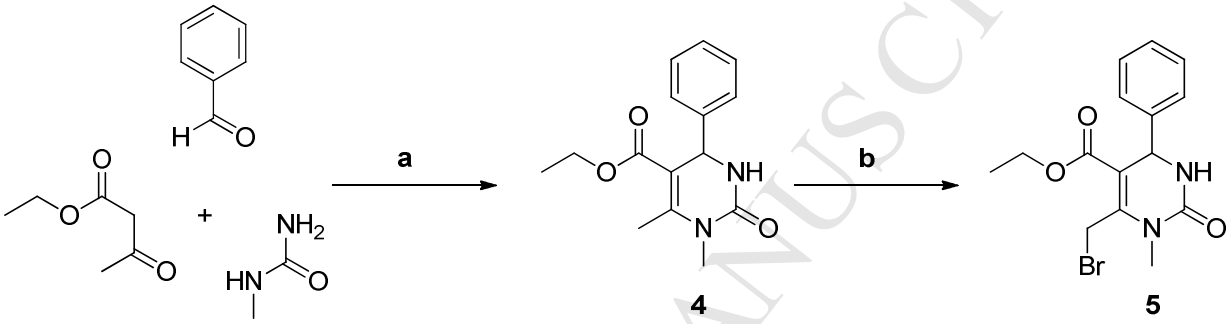

Scheme 1. Synthesis of intermediate **5**. Reagents and conditions: (a) HCl, EtOH, reflux, 3 h, 60%; (b) Br_2, $CHCl_3$, rt, 12 h, 70%.

As shown in scheme 1, the starting DHPM **4** was conveniently prepared *via* multicomponent reaction, of Biginelli type. It involved the cyclocondensation of benzaldehyde, *N*-methyl urea and ethyl acetoacetate in presence of concentrated hydrochloric acid [28]. The intermediate 6-bromomethyl-DHPM **5** was synthesized by treating with Br_2 in $CHCl_3$ [29].

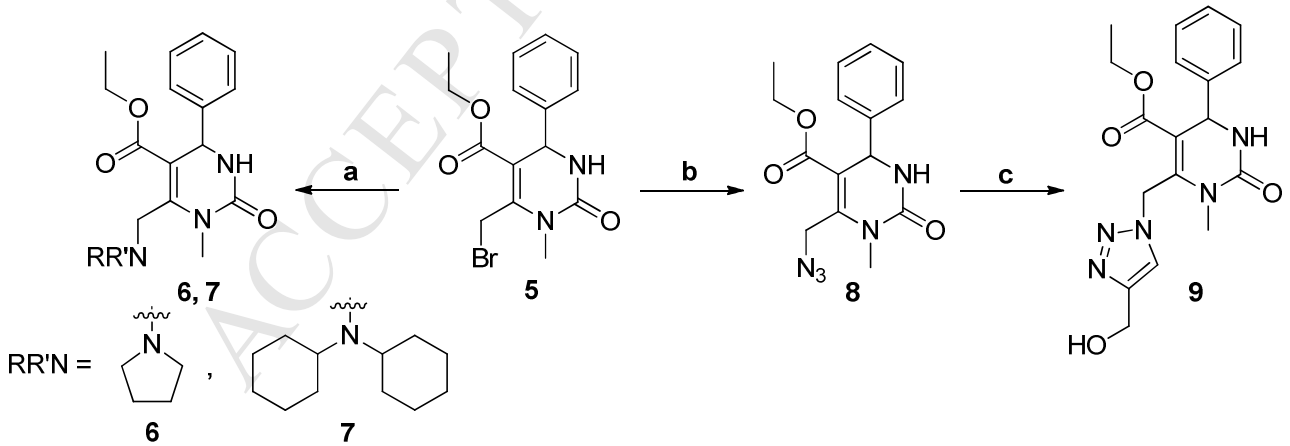

Scheme 2. Synthesis of hybrids **6**–**9**. Reagents and conditions: (a) RR'NH, DMF, K_2CO_3, rt, 8 h; (b) NaN_3, MeOH, rt, 48 h; (c) Propargyl alcohol, Na-ascorbate, $CuSO_4.5\ H_2O$, DMF, rt, 36 h.

Direct amination of intermediate **5** with pyrrolidine and dicyclohexylamine gave hybrids **6** and **7**, respectively (Scheme 2). While, DHPM-1,2,3-triazole hybrid **9** was prepared *via* click chemistry

approach through Cu(I)-catalyzed [3+2] cycloaddition of the known 6-azido-methyl-dihydropyrimidinone **8** [30,31] with propargyl alcohol. The reported $CuSO_4$/sodium ascorbate conditions was utilized to obtain **9** as a single 1,4-disubstituted regioisomer [32,33].

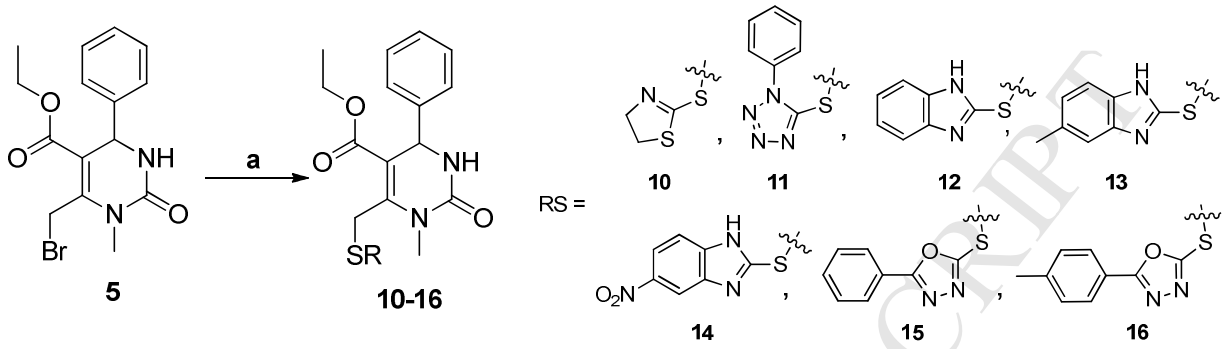

Scheme 3. Synthesis of hybrids **10**–**16**. Reagents and conditions: (a) RSH, DMF, K_2CO_3, rt, 6 h.

A new series of 5-membered heterocycles hybridized with DHPM nucleus at C6 through methyl sulfide bridge **10**–**16** was prepared by direct nucleophilic substitution under basic condition between bromo compound **5** and a wide variety of thiol derivatives (Scheme 3).

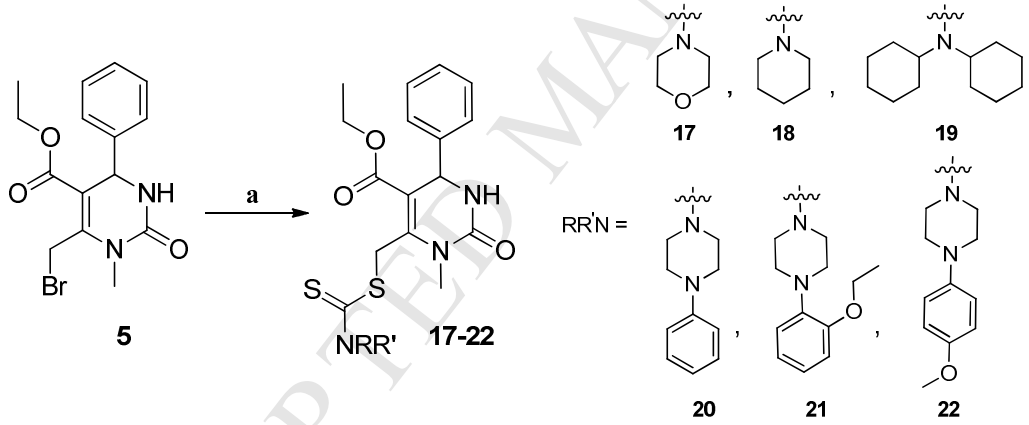

Scheme 4. Synthesis of hybrids **17**–**22**. Reagents and conditions: (a) RR'NH, CS_2, DMF, Na_3PO_4, rt, 4 h.

A series of dithiocarbamate-DHPM derivatives **17**–**22** was synthesized and their structures are shown in scheme 4. The spectroscopic data (^{1}H and ^{13}C-NMR) of the newly synthesized compounds are in agreement with the expected structures as described in the experimental section.

2.2. Biological evaluation

2.2.1. In vitro one-dose anticancer screening

Out of the newly synthesized sixteen target compounds, twelve hybrids namely **6**, **7**, **9**–**12**, **15**, **17**–**20** and **22** (Table 1); were submitted to Developmental Therapeutic Program-National Cancer Institute, Bethesda, USA (www.dtp.nci.nih.gov) to be evaluated for their *in vitro* anticancer activity initially at a single dose (10 μM) towards a panel of NCI 60 cancer cell lines including leukemia, melanoma, lung, colon, CNS, ovarian, renal, prostate and breast cancers. The data are reported as a mean-graph of the percent growth of treated cells compared to the untreated control cells, and presented as percentage growth inhibition (GI %) caused by the test compounds (Table 1).

Data analysis of growth inhibition assay showed that, compounds **19** and **22** have broad spectrum cytotoxic activity with various degrees of growth inhibition against the tested tumor cell lines. Compound **17** showed a potent activity against leukemia cell line K-562 with GI% of 83. Compounds **19** and **20** and **22** have moderate activity against leukemia SR cell line; colon cancer HCT-116, HCT-15 and prostate cancer PC-3 with GI% range of 41-79. Moreover, compound **7** showed moderate activity against prostate cancer PC-3 and breast cancer T-47D with GI% values of 58 and 46, respectively. Compound **10** showed moderate activity against leukemia SR with GI% value of 40.

Table 1. Percentage growth inhibition (GI %) of *in vitro* subpanel tumor cell lines at 10 μM concentration of the selected compounds.

Subpanel cancer cell Lines	% Growth Inhibition (GI%)											
	6	**7**	**9**	**10**	**11**	**12**	**15**	**17**	**18**	**19**	**20**	**22**
Leukemia												
K-562	1	31	10	24	17	10	34	**83**	20	**65**	22	**47**
MOLT-4	4	35	11	19	26	14	29	5	30	**72**	24	**49**
SR	10	20	2	**40**	13	1	16	12	27	**71**	**44**	**63**
HL-60(TB)	-	37	2	10	7	6	11	4	33	**85**	20	32
Non-Small Cell Lung Cancer												
A549/ATCC	-	33	-	16	-	-	5	4	29	**53**	27	33
NCI-H322M	9	5	9	27	18	12	15	18	15	9	15	17
NCI-H522	4	18	5	19	14	3	16	7	25	**42**	28	37
NCI-H460	-	13	-	2	-	-	-	-	10	**88**	12	39
Colon Cancer												
HCT-116	2	33	5	10	12	6	19	6	34	**74**	**41**	**57**
HCT-15	6	11	6	28	8	7	15	7	35	**61**	**48**	**60**
CNS Cancer												
SF-295	9	19	4	10	11	7	14	9	13	**61**	17	15
Melanoma												
LOX IMVI	8	13	7	16	14	11	27	12	11	**67**	13	33
UACC-62	-	23	-	27	17	11	10	16	28	**54**	24	**42**
SK-MEL-5	-	19	-	4	2	-	10	1	25	**86**	23	**51**
Ovarian Cancer												
OVCAR-4	-	26	3	16	4	-	14	-	16	**56**	15	29
NCI/ADR-RES	3	7	4	15	14	6	15	6	12	37	5	13
Renal Cancer												
ACHN	-	13	2	17	3	2	3	7	15	**63**	11	21
CAKI-1	9	30	8	24	14	2	14	-	17	**75**	15	26
UO-31	8	27	7	21	21	4	34	9	29	**56**	37	**55**
Prostate Cancer												
PC-3	-	**58**	-	-	-	8	20	-	27	**79**	**41**	**53**
Breast Cancer												
MCF-7	13	36	12	19	15	14	11	14	12	**54**	15	30
T-47D	1	**46**	1	37	17	-	25	18	**45**	**50**	37	**59**
MDA-MB-468	-	21	-	11	3	1	17	6	20	**53**	14	21

The data showed that compounds bearing different heterocyclic moieties and linked to either -CH_2- (**6**, **7**, **9**) or -CH_2S- (e.g. **10**–**12** and **15**) have week activity towards the tested cell lines. While compounds

bearing dithiocarbamate linkage (e.g. **17**–**20** and **22**) exhibited moderate to high inhibitory activity. Among DHMP-dithiocarbamate hybrids, compound **19** with dicyclohexylamino group exhibited potent and broad activity against several types of cancer cell lines rather than compounds with morpholine, piperidine, or phenyl piperazine moieties. Compound **19** showed a significant anticancer activity against leukemia HL-60(TB), non-small cell lung cancer NCI-H460, and melanoma SK-MEL-5 with GI% 85, 88, and 86, respectively. Removing the dithiocarbamate group from compound **19** gives compound **7** and led to loss of its functional activity.

Figures 4A and 4B show the effect of dithiocarbamate linkage on the functional activity of **19** and **7** towards the 60 NCI cell lines.

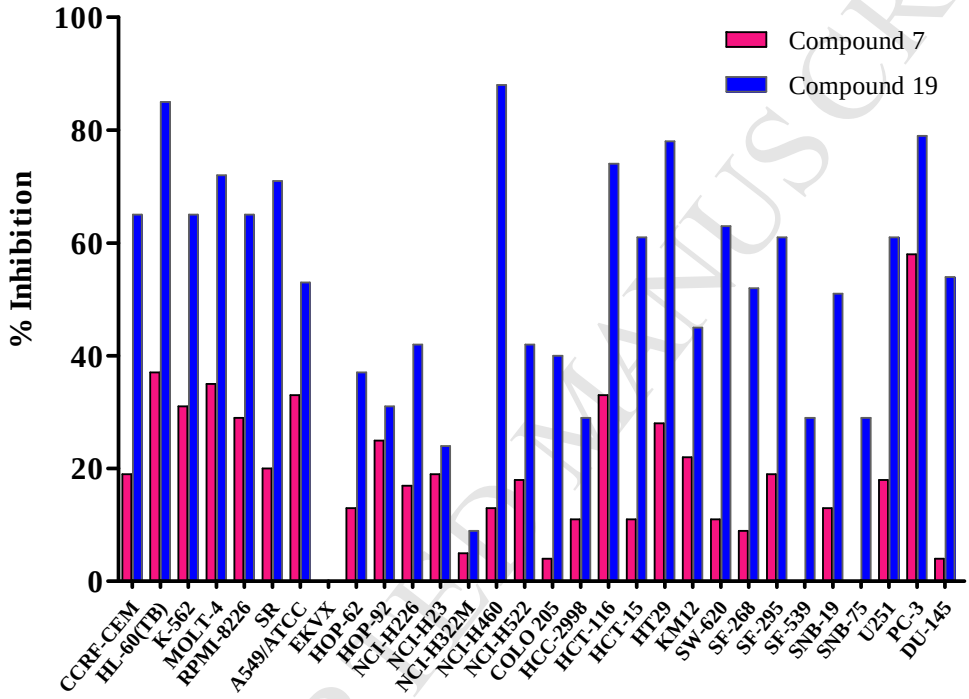

Figure 4A. A comparison between **19** (with dithiocarbamate) and **7** (without dithiocarbamate) (GI %) of *in vitro* subpanel tumor cell lines. **Leukemia:** CCRF-CEM, HL-60(TB), K-562, MOLT-4, RPMI-8226, SR. **Non-Small Cell Lung Cancer:** A549/ATCC, EKVX, HOP-62, HOP-92, NCI-H226, NCI-H23, NCI-H322M, NCI-H460, NCI-H522. **Colon Cancer:** COLO 205, HCC-2998, HCT-116, HCT-15, HT29, KM12, SW-620. **CNS Cancer:** SF-268, SF-295, SF-539, SNB-19, SNB-75, U251. **Prostate Cancer:** PC-3, DU-145.

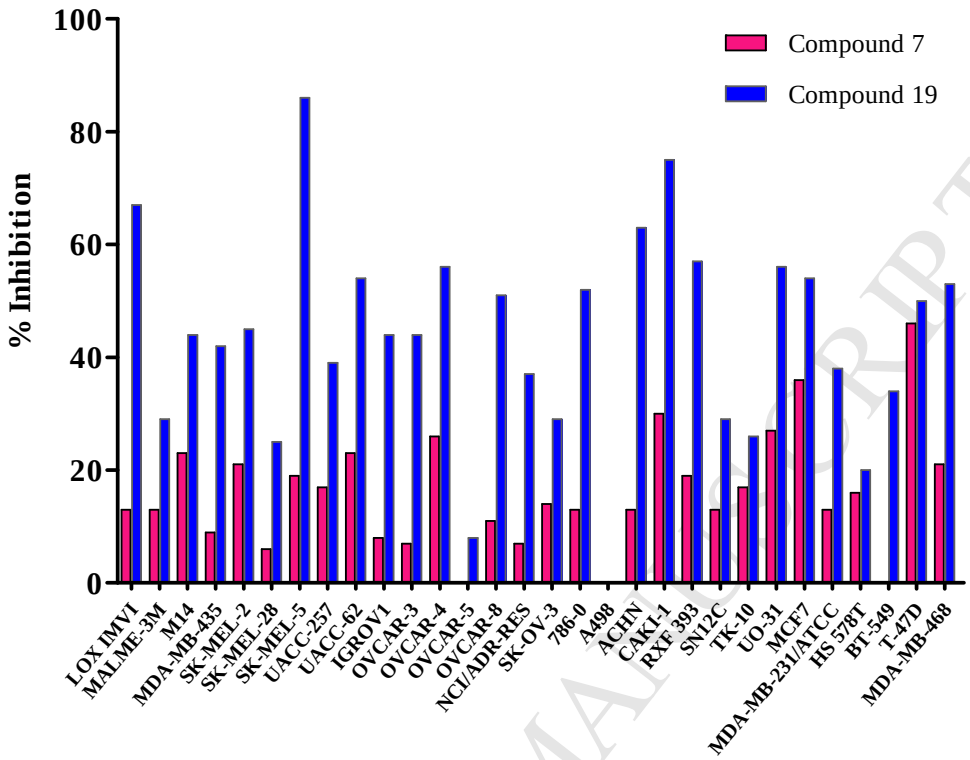

Figure 4B. A comparison between **19** (with dithiocarbamate) and **7** (without dithiocarbamate) (GI %) of *in vitro* subpanel tumor cell lines. **Melanoma:** LOX IMVI, MALME-3M, M14, MDA-MB-435, SK-MEL-2, SK-MEL-28, SK-MEL-5, UACC-257, UACC-62. **Ovarian Cancer:** IGROV1, OVCAR-3, OVCAR-4, OVCAR-5, OVCAR-8, NCI/ADR-RES, SK-OV-3. **Renal Cancer:** 786-0, A498, ACHN, CAKI-1, RXF 393, SN12C, TK-10, UO-31. **Breast Cancer:** MCF7, MDA-MB-231/ATCC, HS 578T, BT-549, T-47D, MDA-MB-468.

The IC_{50} of compounds **13**, **14**, **16** and **21** (that were not selected by NCI) were determined to assess their cytotoxic activity against prostate cancer PC-3, colon cancer HCT-116 and breast cancer MCF-7 (Table 2). The results indicate that compound **14** with nitro group at position 5 is the most active member among benzimidazole thioether series with high cytotoxic activity (IC_{50} = 9.18, 7.29 and 9.39 µM) against PC-3, HCT-116 and MCF-7, respectively. While compound **16** with *p*-tolyl substituent on the oxadiazole ring has moderate activity (IC_{50} = 36.04 and 25.26 µM) against HCT-116 and MCF-7, respectively. Moreover, the IC_{50} data shows that compound **21** exhibits weak inhibitory activities (ranging from 53.75 to 72.29 µM) against the three cell lines. The results were compared with doxorubicin (DOX) as a reference drug.

Table 2. Cytotoxic activity (IC_{50}) of some hybrids against PC-3, HCT-116 and MCF-7 cells.

Compounds	*In vitro* Cytotoxicity IC_{50} (µM)		
	PC-3	HCT-116	MCF-7
13	22.29 ± 2.1	9.50 ± 0.8	19.36 ± 1.8
14	9.18 ± 0.9	7.29 ± 0.6	9.39 ± 1.1
16	61.83 ± 3.8	36.04 ± 2.5	25.26 ± 2.3
21	72.29 ± 4.4	67.60 ± 3.9	53.75 ± 3.5
DOX	8.87 ± 0.6	5.23 ± 0.3	4.17 ± 0.2

Data are shown as means ± SD of three independent experiments.

2.2.2. In vitro cytotoxicity against human normal cells

To investigate whether the synthesized hybrids showed selective cytotoxicity between normal and cancer cells, the most active hybrids **14** and **19** were evaluated against three human normal cell lines including MRC5 (lung), BJ (skin) and WPE1-NA22 (prostate). As shown in figure 5, compounds **14** and **19** exhibited lower toxicity towards MRC5 (IC_{50} = 44.16 and 32.04 µM) in comparison to DOX ((IC_{50} = 14.76 µM). Compound **14** had a lower toxic effect than compound **19** and DOX on the normal BJ. On the other hand, compound **19** induce lower toxicity (IC_{50} = 32.09 µM) on WPE1-NA22 cells as compared with compound **14** and DOX (Table 3).

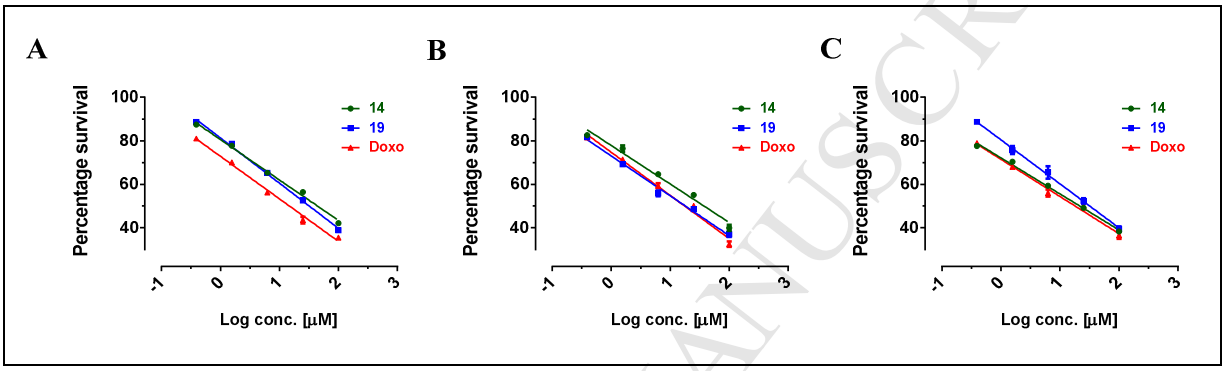

Figure 5. Cytotoxic effect of compounds **14** and **19** in comparison to doxorubicin on lung MRC5 (**A**), skin BJ (**B**) and prostate WPE1-NA22 (**C**) cell lines. Data are shown as means ± SD of three experiments. Data were fitted using linear regression.

Table 3. Cytotoxic activity (IC_{50}) of **14** and **19** hybrids against human normal cells.

Compounds	*In vitro* Cytotoxicity IC_{50} (µM)		
	MRC5	BJ	WPE1-NA22
14	44.16 ± 1.93	37.47 ± 3.43	21.73 ± 1.54
19	32.04 ± 1.0	18.18 ± 1.06	32.09 ± 2.74
DOX	14.76 ± 0.47	17.62 ± 1.01	18.25 ± 2.43

Data are shown as means ± SD of three independent experiments.

2.2.3. Effects on the levels of active caspase-3 and caspase-9

Caspases, cysteine-containing aspartic acid-specific proteases, provide pivotal links in cell regulatory networks controlling cell death. Caspase-3 is a key executioner protease which is activated by upstream initiator caspases as caspase-9 [34,35].

Herein, the study was further extended to investigate the ability of compound **19** to provoke apoptosis in A549 lung cell line. Treatment of A549 cell line with compound **19** significantly increased the expression levels of active caspases-3 and caspases-9 by about 10 and 100 folds, respectively, in comparison to the control, 5-fluorouracil (5-FU) (Table 4).

Table 4. Effect of hybrid **19** on caspase-3 and caspase-9 enzyme assay in A549 cells.

Compound	Conc. (μM)	Caspase-3 ng/mL	Caspase-9 ng/mL
Control	-	53.45	0.1726
5-FU	7.4	582.1	16.84
19	3.04	560.4	18.14

2.2.4. Effect on cell cycle progression

To gain further evidence regarding the role of the synthesized hybrids in growth inhibition of cancer cells, measuring of cell cycle arrest and induction of apoptosis was performed in different phases. Thus, we started to investigate the effect of compound **19** on cell cycle distribution in A549 cells. The cells were treated with compound **19** at a concentration of 2 μM for 24 h, stained with propidium iodide (PI), and analyzed by flow cytometer (FCM) according to the literature. Normal lymphocyte DNA was used to set diploid G0-G1 phase and the untreated cells exhibited significant arrest in synthetic S-phase. The results showed that cells were arrested in G2-M phase of the cell cycle at 24 h by 12.4% (Table 5). Additionally, the hybrid **19** at 24 h induced block in G0-G1 phase by 58.3% as compared to that of positive control 5-FU (47.4%). The induced apoptosis was determined by measuring the percent of cells stalled in the pre-G1 peak: 7.4 and 15.5% of cells were found in the pre-G1 peak after 48 h exposure of **19** and 5-FU, respectively compared to the untreated A549 cells.

Table 5. Effect of hybrid **19** on the cell cycle progression in A549 cells using flow cytometry.

Compound	Cell cycle distribution (%)			
	G0/G1	S	G2/M	Pre/G1
Control	67.62	25.26	6.2	0.92
5-FU	47.36	16.08	21.04	15.52
19	58.25	21.95	12.41	7.39

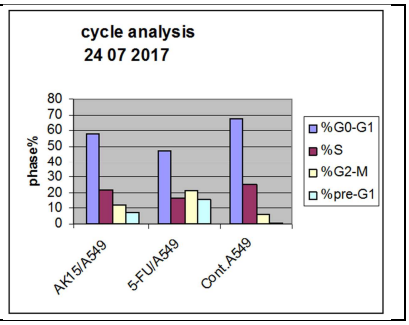

2.2.5. Detection of apoptosis

Extrinsic and intrinsic apoptosis in A549 cells induced by hybrid **19** were also evaluated by Annexin V and PI staining. In this study A549 cells were incubated with **19** at 2 μM concentration for 24 h. Compound **19** was found to induce early apoptosis (3.27%) in A549 at 24 h and enhanced late apoptotic induction (3.31%) by 10 folds over the control. Cumulatively, **19** induced apoptosis with 6.6%, and the results were compared with 5-FU (Figure 6B). This finding is consistent with the data obtained from cell cycle analysis in figure 6A.

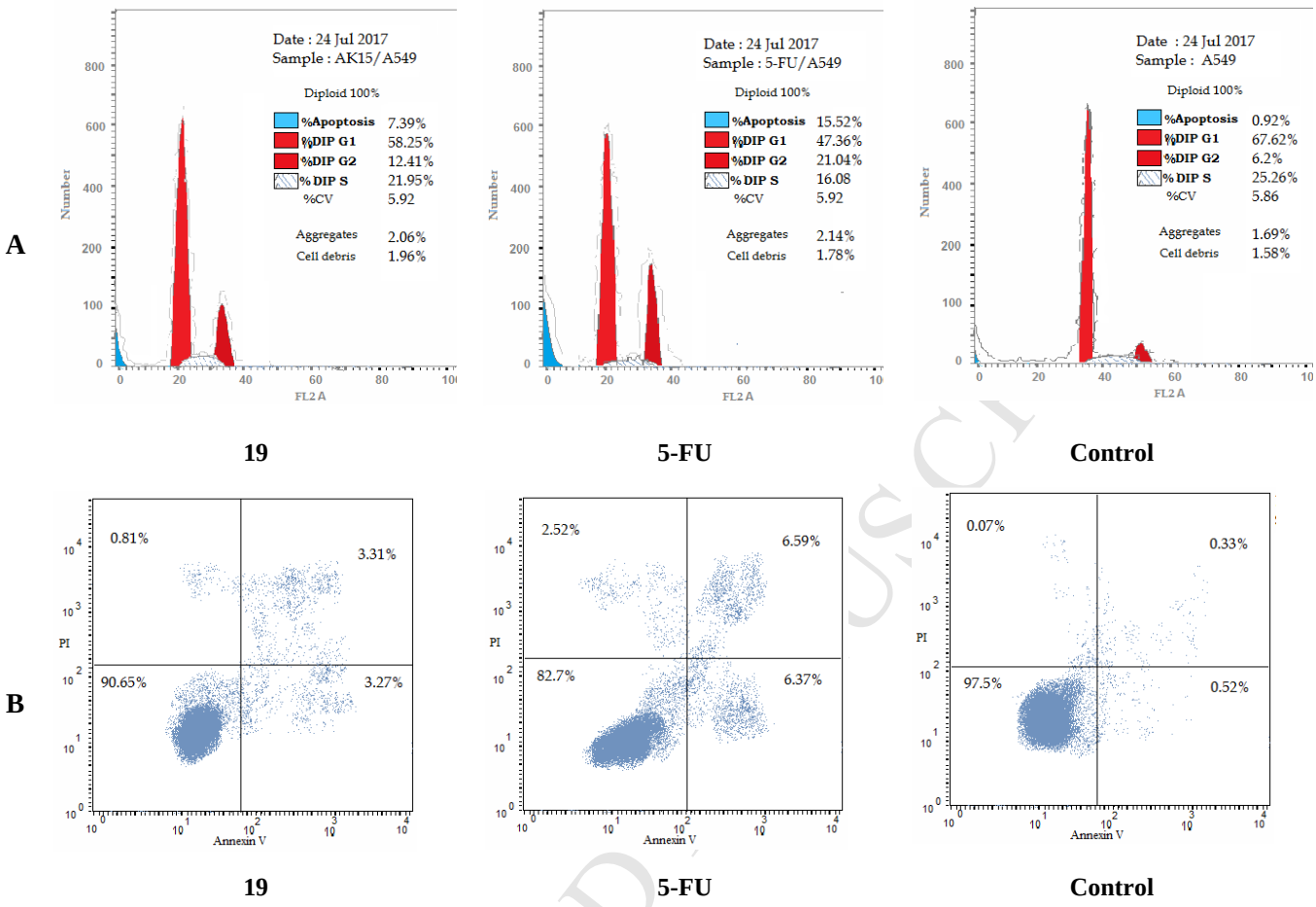

Figure 6. **A)** Effect of compound **19** on the cell cycle distribution of A549 cell line. **B)** Apoptosis effect on A549 cell line induced by compound **19**.

2.2.6. VEGFR-2 and mTOR enzyme assay inhibition

The most active anticancer agents (**14** and **19**) were screened as inhibitors of VEGFR-2 and mTOR and the IC_{50} results are shown in table 6. Compounds **14** and **19** showed high inhibitory activity with IC_{50} values of 1.20 µM for **14** and 1.97 µM for **19** with 75.99% and 68.52% VEGFR-2 inhibition, respectively in comparison to the reference drug, sorafinib, with IC_{50} of 0.32 µM, and 91.49% VEGFR-2 inhibition (Table 6). In addition, both compounds showed high inhibitory activity against mTOR with IC_{50} values of 0.72 µM for **14** and 0.64 µM for **19** with % inhibition of 84.58% and 86.57%, respectively in comparison to the reference drug, rapamycin, with IC_{50} of 0.43 µM, and 94.88% mTOR inhibition (Table 6). These results indicate that DHPM derivatives contribute more to the interaction with mTOR enzyme rather than VEGFR-2 enzyme.

Table 6. Inhibitory activities and cytotoxicity of **14** and **19** (IC_{50} µM) against VEGFR-2 and mTOR enzymes against Hela cell line.

Compound	IC_{50} (µM) Hela cells	VEGFR-2		mTOR	
		% inhibition	IC_{50} (µM)	% inhibition	IC_{50} (µM)
14	1.40±0.08	75.99	1.2	84.58	0.72
19	1.85±0.1	68.52	1.97	86.57	0.64
Sorafinib	0.64±0.05	91.49	0.32	-	-
Rapamycin	0.77±0.08	-	-	94.88	0.43

2.2.7. Physicochemical properties and Lipinski's rule of five

The most active synthesized compound **19** was evaluated to test its compliance to the Lipinski's rule of five in comparison to rapamycin. Calculations were performed by SwissADME web service [36]. Molecules violating more than one of these rules may have problems with bioavailability. Predictions of ADME properties for the studied compound **19** are given in table 7. The results showed that compound **19** complies with these rules, while rapamycin does not, suggesting that compound **19** would possess drug-like characters. Predictions of water solubility of **19** and rapamycin revealed that both compounds have poor solubility, however, the topological polar surface area (TPSA) value for **19** is 119.27 in comparison to rapamycin (TPSA = 195.43) and theoretically it may confer better passive oral absorption for **19** than rapamycin.

Table 7. Solubility, topological surface area and calculated Lipinski's rule of five for compound **19** and rapamycin.

Compound	Log *S*[a]	TPSA[b]	MW[c]	Mlog *P*[d]	nHBA[e]	nHBD[f]	nRB[g]	nVio[h]
19	-6.15	119.27	529.76	3.72	3	1	10	1
Rapamycin	-8.90	195.43	914.17	1.00	13	3	6	2

[a]Solubility parameter. [b]Topological polar surface area (Å²). [c]Molecular weight. [d]Lipophilicity parameter. [e]Number of hydrogen bond acceptors. [f]Number of hydrogen bond donors. [g]Number of rotatable bonds. [h]Number of violations to Lipinski's rule of five.

3. Conclusion

Several hybrids of DHPM with *N*-hterocyclic moieties were synthsized and evaluated for their anticancer activity against a panel of cancer cell lines according to NCI (USA) protocol. DHPM with dithiocarbamate moiety **19** was identified as the most promising anticancer candidate against NCI-H460, SK-MEL-5, and HL-60(TB). The inhibitory activities against VEGFR-2 and mTOR as well as the induction of apoptosis of **19** were also investigated.

4. Experimental

4.1. Chemistry

4.1.1. General

Melting points were measured using Fischer-John device and are uncorrected. IR spectra were recorded on Nicolet IS 10 FT-IR spectrometer in KBr discs. The ^{1}H NMR spectra were recorded on Bruker 200 MHz (for **6** and **10**), Bruker 400 MHz (for **11**–**19**, **22**) or Jeol 500 MHz (for **7**, **9**, **20**, **21**) NMR spectrometer, while the ^{13}C NMR spectra were recorded on Bruker 100 MHz (for **6**, **10**–**19**, **22**) or Jeol 125 MHz (for **7**, **9**, **20**, **21**) NMR spectrometer, with the deuterated solvent as the lock and residual solvent as the internal refrence. All chemical shift values, coupling constants *J* and the multiplicity (s = singlet, d = doublet, t = triplet, m = multiplet, br = broad) are quoted in ppm and in Hz, respectively. The intermediates **4** [28], **5** [29] and **8** [30,31] were prepared according to the described method. All chemicals and reagents were commercially availble from Aldrich, Fluca or Merck.

*4.1.2. Ethyl 1,6-dimethyl-2-oxo-4-phenyl-1,2,3,4-tetrahydropyrimidine-5-carboxylate (**4**)*

To a mixture of benzaldehyde (10 g, 2 mmol), ethyl acetoacetate (12.26 g, 2.4 mmol) and N-methyl urea (8.38 g, 2.4 mmol) in EtOH (40 mL), concentrated hydrochloric acid (0.5 mL) was added. The mixture was stirred under reflux for 3 h. After cooling the solution to 0 °C for 1 h, the formed precipitate was collected, dried and recrystallized from EtOH to give compound **4** (15.6 g, 60%) with m.p. 176–177 °C (lit. 175–176 ºC) [28].

*4.1.3. Ethyl 6-(bromomethyl)-1-methyl-2-oxo-4-phenyl-1,2,3,4-tetrahydro pyrimidine-5-carboxylate (**5**)*

A solution of Bromine (1.6 g, 0.01 mol) in $CHCl_3$ (50 mL) was slowly added to a stirred solution of **4** (2.47 g, 0.01 mol) in $CHCl_3$ (30 mL) at 4 °C over 6 h. The reaction mixture was warmed to rt, stirred for 12 h, and the solvent was removed under reduced pressure. The formed precipitate was crystallized from EtOH to give compound **5** (2.22 g, 70%) with m.p. 170–171 °C (lit. 170 °C) [29].

*4.1.4. General procedure for preparation compounds **6** and **7**.*

To a solution of compound **5** (0.35 g, 1 mmol) in DMF (5 mL), the appropriate amine (1 mmol) and K_2CO_3 (0.14 g, 1 mmol) was added and the mixture was stirred for 8 h at room temperature. The reaction mixture was poured into a mixture of ice and water and stirred for 10 min. The separated solid was filtered, washed with cold water and recrystallized from EtOH to afford pure product of compounds **6** and **7**.

*4.1.4.1. Ethyl 1-methyl-2-oxo-4-phenyl-6-(pyrrolidin-1-ylmethyl)-1,2,3,4-tetrahydropyrimidine-5-carboxylate (**6**)*

Yield (0.23 g, 67%) as white solid with m.p. 169–170 °C. IR (KBr) (υ, cm^{-1}): 1508 (C=C str.), 1637 (C=O amide), 1725 (C=O ester), 2977 (C-H Ar. str.), 3241 (NH). ^{1}H-NMR (200 MHz, DMSO): 1.16 (3H, t, *J* = 7.1 Hz, CH_3-CH_2), 1.65-1.71 (4H, m, pyrrolidine-2CH_2), 2.52 (4H, dd, *J* = 3.6, 1.8 Hz, pyrrolidine-2CH_2), 3.25 (3H, s, N-CH_3), 3.89 (1H, d, *J* = 13.2 Hz, CH_2-N), 4.01 (1H, d, *J* = 13.2 Hz, CH_2-N), 4.08 (2H, q, *J* = 7.1 Hz, CH_2-CH_3), 5.20 (1H, d, *J* = 3.6 Hz, pyrimidine-CH), 7.23 (1H, m, Ar-H), 7.27-7.30 (2H, m, Ar-H), 7.31-7.40 (2H, m, Ar-H), 7.98 (1H, d, *J* = 3.6 Hz, NH). ^{13}C-NMR (100 MHz, DMSO): 14.0, 24.3, 29.6, 52.3, 55.1, 57.6, 60.2, 105.3, 126.4, 127.6, 128.6, 143.5, 147.8, 153.1, 165.6. EI-MS: m/z (%): 343 (M^+, 72). Anal. Calcd. for $C_{19}H_{25}N_3O_3$ (343.19): C, 66.45; H, 7.34; N, 12.24. Found: C, 66.42; H, 7.35; N, 12.23.

*4.1.4.2. Ethyl 6-((dicyclohexylamino)methyl)-1-methyl-2-oxo-4-phenyl-1,2,3,4-tetrahydropyrimidine-5-carboxylate (**7**)*

Yield (0.24 g, 54%) as white solid with m.p. 187–188 °C. ^{1}H-NMR (500 MHz, DMSO): 0.94-1.11 (6H, m, cyclohexyl-H), 1.14 (3H, t, *J* = 6.9 Hz, CH_3-CH_2), 1.22-1.39 (5H, m, cyclohexyl-H), 1.47-1.55 (2H, m, cyclohexyl-H), 1.55-1.64 (5H, m, cyclohexyl-H), 1.64-1.1.75 (4H, m, cyclohexyl-H), 3.27 (3H, s, N-CH_3), 3.88 (1H, d, *J* = 13.4 Hz CH_2-N), 4.07 (2H, q, *J* = 6.9 Hz, CH_2-CH_3), 4.21 (1H, d, *J* = 13.4 Hz CH_2-N), 5.19 (1H, d, *J* = 2.8 Hz, pyrimidine-CH), 7.21 (2H, d, *J* = 7.1 Hz, Ar-H), 7.25 (1H, m, Ar-H), 7.32 (2H, t, *J* = 7.1 Hz, Ar-H), 7.91 (1H, d, *J* = 2.8 Hz, NH). ^{13}C-NMR (125 MHz, DMSO): 13.9, 24.7, 25.8, 29.6, 30.1, 45.5, 52.4, 60.2, 62.3, 106.1, 126.2, 127.2, 128.8, 143.3, 147.7, 153.1, 164.9. EI-MS: m/z (%): 453(M^+, 66). Anal. Calcd. for $C_{27}H_{39}N_3O_3$ (453.30): C, 71.49; H, 8.67; N, 9.26. Found: C, 71.45; H, 8.70; N, 9.24.

*4.1.4.3 Ethyl 6-(azidomethyl)-1-methyl-2-oxo-4-phenyl-1,2,3,4-tetrahydropyrimidine-5-carboxylate (**8**)*[30,31]

Sodium azide (0.1 g, 1.5 mmol) was added to a solution of compound **5** (0.35 g, 1 mmol) in MeOH (10 mL) and the mixture was stirred at room temperature for 48 h. After completion of the reaction, the solvent was evaporated under reduced pressure and the produced product was washed with water, dried to afford white solid (0.23 g, 75 % yield) and used without further purification in the next step.

*4.1.6. Ethyl 6-((4-(hydroxymethyl)-1H-1,2,3-triazol-1-yl)methyl)-1-methyl-2-oxo-4-phenyl-1,2,3,4-tetrahydropyrimidine-5-carboxylate (**9**)*

To a solution of azide **8** (0.32 g, 1 mmol) in DMF (5 mL), propargyl alcohol (0.06 g, 1 mmol), $CuSO_4$.5 H_2O (5 mg, 2 mol%), and sodium ascorbate (40 mg, 0.2 mmol) were added and the mixture was stirred at room temperature for 36 h. The reaction mixture was poured into a mixture of ice and water and stirred for 2 h. The separated solid was collected by filtration, washed with water, dried and recrystallized from a mixture of EtOH and water to afford compound **9** (0.27 g, 72% yield) as beige solid with m.p. 172-173 °C. IR (KBr) (υ, cm^{-1}): 1498 (C=C str.), 1644 (C=O amide), 1723 (C=O ester), 2968 (C-H Ar. str.), 3211 (O-H str.), 3257 (NH). ^{1}H-NMR (500 MHz, DMSO): 1.11 (3H, t, *J* = 7.1 Hz, CH_3-CH_2), 3.08 (3H, s, N-CH_3), 4.08 (2H, q, *J* = 7.1 Hz, CH_2-CH_3), 4.52 (2H, d, *J* = 5.6 Hz, CH_2OH), 5.20 (1H, t, *J* = 5.6 Hz, OH), 5.24 (1H, d, *J* = 3.8 Hz, pyrimidine-CH), 5.81 (1H, d, *J* = 15.0 Hz, CH_2-N), 6.00 (1H, d, , *J* = 15.0 Hz, CH_2-N), 7.26-7.31 (3H, m, Ar-H), 7.33-7.36 (2H, m, Ar-H), 7.93 (1H, s, triazole-CH), 8.14 (1H, d, *J* = 3.8 Hz, NH). ^{13}C-NMR (125 MHz, DMSO): 14.3, 30.0, 46.6, 53.0, 55.5, 60.9, 105.4, 123.1, 126.7, 128.2, 129.1, 143.5, 145.6, 148.8, 153.4, 165.4. EI-MS: m/z (%): 371 (M^+, 34). Anal. Calcd. for $C_{18}H_{21}N_5O_4$ (371.16): C, 58.21; H, 5.70; N, 18.86. Found: C, 58.22; H, 5.75; N, 18.88.

*4.1.5. General procedure for preparation compounds **10**–**16**.*

To a solution of compound **5** (0.35 g, 1 mmol) in DMF (5 mL) the appropriate thiol (1 mmol) and K_2CO_3 (0.14 g, 1 mmol) were added and the mixture was stirred for 6 h at room temperature. The reaction mixture was poured into crushed ice and stirred for 1 h. The separated solid was filtered, washed with ice-cold water and recrystallized from EtOH to afford compounds **10**–**16**.

*4.1.7.1. Ethyl 6-((4,5-dihydrothiazol-2-ylthio)methyl)-1-methyl-2-oxo-4-phenyl-1,2,3,4-tetrahydropyrimidine-5-carboxylate (**10**)*

Yield (0.24 g, 62%) as white solid with m.p. 150–151 °C. ^{1}H-NMR (200 MHz, DMSO): 1.13 (3H, t, *J* = 7.1 Hz, CH_3-CH_2), 3.16 (3H, s, N-CH_3), 3.49 (2H, t, *J* = 8.0 Hz, thiazole-CH_2), 4.06 (2H, q, *J* = 7.1 Hz, CH_2-CH_3), 4.16 (2H, t, *J* = 8.0 Hz, thiazole-CH_2), 4.67 (1H, d, *J* = 13.1 Hz, S-CH_2), 4.79 (1H, d, *J* = 13.1 Hz, S-CH_2), 5.14 (1H, d, *J* = 3.8 Hz, pyrimidine-CH), 7.19-7.23 (2H, m, Ar-H), 7.26 (1H, m, Ar-

H), 7.31-7.36 (2H, m, Ar-H), 8.07 (1H, d, *J* = 3.8 Hz, NH). ^{13}C-NMR (100 MHz, DMSO): 13.9, 29.6, 30.3, 35.5, 52.3, 59.6, 60.2, 105.9, 126.1, 127.6, 128.7, 143.2, 147.6, 153.1, 163.9, 166.0. EI-MS: m/z (%): 391 (M^+, 23). Anal. Calcd. for $C_{18}H_{21}N_3O_3S_2$ (391.10): C, 55.22; H, 5.41; N, 10.73. Found: C, 55.25; H, 5.38; N, 10.77.

*4.1.5.1. Ethyl 1-methyl-2-oxo-4-phenyl-6-((1-phenyl-1H-tetrazol-5-ylthio)methyl)-1,2,3,4-tetrahydropyrimidine-5-carboxylate (**11**)*
Yield (0.23 g, 52%) as white solid with m.p. 109–110 °C. ^{1}H-NMR (400 MHz, $CDCl_3$): 1.20 (3H, t, *J* = 7.1 Hz, CH_3-CH_2), 3.41 (3H, s, N-CH_3), 4.15 (2H, q, *J* = 7.1 Hz, CH_2-CH_3), 4.94 (1H, d, *J* = 12.8 Hz, CH_2-S), 5.15 (1H, d, *J* = 12.8 Hz, CH_2-S), 5.39 (1H, s, Pyrimidine-CH), 5.79 (1H, s, NH), 7.24-7.29 (2H, m, Ar-H), 7.30-7.34 (3H, m, Ar-H), 7.59 (5H, s, Ar-H). ^{13}C-NMR (100 MHz, DMSO): 13.9, 29.6, 30.3, 52.3, 60.2, 105.8, 124.1, 126.4, 127.6, 128.5, 128.9, 129.0, 134.2, 143.3, 147.6, 153.1, 156.7, 166.0. EI-MS: m/z (%): 450 (M^+, 68). Anal. Calcd. for $C_{22}H_{22}N_6O_3S$ (450.15): C, 58.65; H, 4.92; N, 18.65. Found: C, 58.61; H, 4.88; N, 18.63.

*4.1.5.2. Ethyl 6-((1H-benzo[d]imidazol-2-ylthio)methyl)-1-methyl-2-oxo-4-phenyl-1,2,3,4-tetrahydropyrimidine-5-carboxylate (**12**)*
Yield (0.27 g, 65%) as white solid with m.p. 134–135 °C. ^{1}H-NMR (400 MHz, DMSO): 1.10 (3H, t, *J* = 7.1 Hz, CH_3-CH_2), 3.21 (3H, s, N-CH_3), 4.03 (2H, q, *J* = 7.1 Hz, CH_2-CH_3), 4.81 (1H, d, *J* = 13.0 Hz, CH_2-S), 5.00 (1H, d, *J* = 13.0 Hz, CH_2-S), 5.15 (1H, d, *J* = 3.8 Hz, pyrimidine-CH), 7.12-7.16 (2H, m, Ar-H), 7.21-7.29 (3H, m, Ar-H), 7.31-7.35 (2H, m, Ar-H), 7.39 (1H, d, *J* = 7.0 Hz, Ar-H), 7.53 (1H, d, *J* = 6.3 Hz, Ar-H), 8.07 (1H, d, *J* = 3.8 Hz, pyrimidine-NH), 12.68 (1H, s, benzimidazole-NH). ^{13}C-NMR (100 MHz, DMSO): 13.9, 29.6, 29.7, 52.4, 60.2, 105.4, 110.6, 117.6, 121.3, 122.0, 126.1, 127.6, 128.5, 128.6, 135.5, 143.3, 143.5, 147.8, 153.1, 164.9. EI-MS: m/z (%): 422 (M^+, 15). Anal. Calcd. for $C_{22}H_{22}N_4O_3S$ (422.14): C, 62.54; H, 5.25; N, 13.26. Found: C, 62.52; H, 5.26; N, 13.25.

*4.1.5.3. Ethyl 1-methyl-6-((5-methyl-1H-benzo[d]imidazol-2-ylthio)methyl)-2-oxo-4-phenyl-1,2,3,4-tetrahydropyrimidine-5-carboxylate (**13**)*
Yield (0.26 g, 61%) as white solid with m.p. 98–99 °C. IR (KBr) (υ, cm^{-1}): 1487 (C=C str.), 1640 (C=O amide), 1721 (C=O ester), 3021 (C-H Ar. str.), 3248 (NH), 3315 (NH). ^{1}H-NMR (400 MHz, $CDCl_3$): 1.14 (3H, t, *J* = 7.1 Hz, CH_3-CH_2), 2.44 (3H, s, benzimidazole-CH_3), 3.35 (3H, s, N-CH_3), 4.06 (2H, q, *J* = 7.1 Hz, CH_2-CH_3), 4.79 (2H, s, CH_2-S), 5.34 (1H, d, *J* = 3.0 Hz, pyrimidine-CH), 5.71 (1H, d, *J* = 3.0 Hz, pyrimidine-NH), 7.03 (1H, dd, *J* = 6.7, 6.7 Hz, Ar-H), 7,09 (1H, s, Ar-H), 7.16-7.22 (2H, m, Ar-H), 7.23-6.26 (3H, m, Ar-H), 7.53 (1H, m, Ar-H), 10.25 (1H, s, benzimidazole-NH). ^{13}C-NMR (100 MHz, DMSO): 13.7, 21.3, 29.6, 30.2, 52.4, 60.2, 105.6, 111.0, 115.4, 121.3, 126.4, 127.3, 128.2, 128.6, 132.6, 135.9, 143.0, 143.5, 147.8, 153.1, 165.0. EI-MS: m/z (%): 436 (M^+, 81). Anal. Calcd. for $C_{23}H_{24}N_4O_3S$ (436.16): C, 63.28; H, 5.54; N, 12.83. Found: C, 63.26; H, 5.58; N, 12.82.

*4.1.5.4. Ethyl 1-methyl-6-((5-nitro-1H-benzo[d]imidazol-2-ylthio)methyl)-2-oxo-4-phenyl-1,2,3,4-tetrahydropyrimidine-5-carboxylate (**14**)*
Yield (0.31 g, 67%) as light brown solid with m.p. 121–122 °C. ^{1}H-NMR (400 MHz, $CDCl_3$): 1.21 (3H, t, *J* = 7.0 Hz, CH_3-CH_2), 3.41 (3H, s, N-CH_3), 4.18 (2H, q, *J* = 7.0 Hz, CH_2-CH_3), 4.87 (1H, s, CH_2-S), 4.98 (1H, s, CH_2-S), 5.39 (1H, s, pyrimidine-CH), 5.94 (1H, s, pyrimidine-NH), 7.16-7.24 (2H, m, Ar-H), 7.28-7.42 (3H, m, Ar-H), 7.44-7.60 (1H, m, Ar-H), 8.15 (1H, d, *J* = 8.4 Hz, Ar-H), 8.39 (1H, s, Ar-H). ^{13}C-NMR (100 MHz, DMSO): 13.8, 29.6, 29.9, 52.3, 60.2, 105.7, 111.2, 113.1, 117.2, 126.6, 127.6, 128.3, 128.5, 135.8, 143.4, 143.4, 143.5, 147.7, 153.1, 165.2. EI-MS: m/z (%): 467 (M^+, 59). Anal. Calcd. for $C_{22}H_{21}N_5O_5S$ (467.13): C, 56.52; H, 4.53; N, 14.98. Found: C, 56.49; H, 4.56; N, 15.01.

*4.1.5.5. Ethyl 1-methyl-2-oxo-4-phenyl-6-((5-phenyl-1,3,4-oxadiazol-2-ylthio)methyl)-1,2,3,4-tetrahydropyrimidine-5-carboxylate (**15**)*

Yield (0.3 g, 68%) as light brown solid with m.p. 79–80 °C. ^{1}H-NMR (400 MHz, $CDCl_3$): 1.19 (3H, t, *J* = 7.1 Hz, CH_3-CH_2), 3.44 (3H, s, N-CH_3), 4.13 (2H, q, *J* = 7.1 Hz, CH_2-CH_3), 4.85 (1H, d, *J* = 11.5 Hz, CH_2-S), 4.98 (1H, d, *J* = 11.5 Hz, CH_2-S), 5.42 (1H, s, pyrimidine-CH), 5.67 (1H, s, NH), 7.26-7.39 (6H, m, Ar-H), 7.49-7.58 (2H, m, Ar-H), 7.89 (1H, d, *J* = 8.0 Hz, Ar-H), 8.01(1H, d, *J* = 7.1 Hz, Ar-H). ^{13}C-NMR (100 MHz, DMSO): 13.7, 29.6, 30.3, 52.3, 60.2, 106.0, 120.3, 126.2, 126.3, 127.6, 128.1, 128.7, 142.7, 143.4, 147.8, 153.4, 161.5, 165.2, 166.6. EI-MS: m/z (%): 450 (M^+, 100). Anal. Calcd. for $C_{23}H_{22}N_4O_4S$ (450.14): C, 61.32; H, 4.92; N, 12.44. Found: C, 61.30; H, 4.96; N, 12.43.

*4.1.5.6. Ethyl 1-methyl-2-oxo-4-phenyl-6-((5-p-tolyl-1,3,4-oxadiazol-2-ylthio)methyl)-1,2,3,4-tetrahydropyrimidine-5-carboxylate (**16**)*

Yield (0.32 g, 70%) as beige solid with m.p. 132–133 °C. ^{1}H-NMR (400 MHz, $CDCl_3$): 1.10 (3H, t, *J* = 7.1 Hz, CH_3-CH_2), 2.36 (3H, s, phenyl-CH_3), 3.35 (3H, s, N-CH_3), 4.03 (2H, q, *J* = 7.1 Hz, CH_2-CH_3), 4.74 (1H, d, *J* = 12.8 Hz, CH_2-S), 4.88 (1H, d, *J* = 12.8 Hz, CH_2-S), 5.32 (1H, s, pyrimidine-CH), 5.50 (1H, s, NH), 7.18-7.24 (7H, m, Ar-H), 7.80 (2H, d, *J* = 8.2 Hz, Ar-H). ^{13}C-NMR (100 MHz, DMSO): 13.7, 21.2, 29.6, 30.3, 52.3, 60.2, 105.8, 120.2, 126.1, 126.4, 127.6, 128.6, 130.0, 142.4, 143.1, 147.6, 153.1, 161.3, 164.8, 166.2. EI-MS: m/z (%): 464 (M^+, 47). Anal. Calcd. for $C_{24}H_{24}N_4O_4S$ (464.15): C, 62.05; H, 5.21; N, 12.06. Found: C, 62.01; H, 5.23; N, 12.10.

*4.1.6. General procedure for preparation compounds (**17**–**22**)*

A mixture of the appropriate amine (1.5 mmol), carbon disulfide (0.45 mL, 7.5 mmol) and anhydrous sodium phosphate (0.33 g, 2.0 mmol) in DMF (8 mL) was stirred at room temperature for 30 min. Compound **5** (0.53 g, 1.5 mmol) was added, and stirred at room temperature for 4 h. The reaction mixture was poured into a mixture of ice and water (60 mL). The separated solid was collected by filtration, and recrystallized from a mixture of DMF and water to afford compounds **17**–**22**.

*4.1.6.1. Ethyl 1-methyl-6-((morpholine-4-carbonothioylthio)methyl)-2-oxo-4-phenyl-1,2,3,4-tetrahydropyrimidine-5-carboxylate (**17**)*

Yield (0.37 g, 57%) as off-white solid with m.p. 120–121 °C. IR (KBr) (υ, cm^{-1}): 850 (C-S str.), 1070 (C=S str.), 1512 (C=C str.), 1638 (C=O amide), 1720 (C=O ester), 2965 (C-H Ar. str.), 3244 (NH). ^{1}H-NMR (400 MHz, DMSO): 1.12 (3H, t, *J* = 7.1 Hz, CH_3-CH_2), 3.14 (3H, s, N-CH_3), 3.67 (4H, s, morpholine-2CH_2), 3.93 (2H, s, morpholine-CH_2), 4.05 (2H, q, *J* = 7.1 Hz, CH_2-CH_3), 4.22 (2H, s, morpholine-CH_2), 4.75 (1H, d, *J* = 12.5 Hz, CH_2-S), 4.88 (1H, d, *J* = 12.5 Hz, CH_2-S), 5.17 (1H, d, *J* = 3.6 Hz, pyrimidine-CH), 7.24 (2H, dd, *J* = 7.4, 7.4 Hz, Ar-H), 7.26-7.30 (1H, m, Ar-H), 7.34 (2H, dd, *J* =7.4,7.4 Hz, Ar-H), 8.10 (1H, d, *J* = 3.6 Hz, NH). ^{13}C-NMR (100 MHz, DMSO): 13.9, 29.6, 35.6, 51.5, 52.5, 60.2, 65.6, 106.1, 126.2, 127.6, 128.6, 143.3, 146.3, 152.9, 164.7, 193.7. EI-MS: m/z (%): 435 (M^+, 55). Anal. Calcd. for $C_{20}H_{25}N_3O_4S_2$ (435.13): C, 55.15; H, 5.79; N, 9.65. Found: C, 55.12; H, 5.78; N, 9.65.

*4.1.6.2. Ethyl 1-methyl-2-oxo-4-phenyl-6-((piperidine-1-carbonothioylthio)methyl)-1,2,3,4-tetrahydropyrimidine-5-carboxylate (**18**)*

Yield (0.4 g, 62%) as white solid with m.p. 169–170 °C. ^{1}H-NMR (400 MHz, DMSO): 1.12 (3H, t, *J* = 7.1 Hz, CH_3-CH_2), 1.53-1.63 (4H, m, piperidine-2CH_2),1.63-1.70 (2H, m, piperidine-CH_2), 3.13 (3H, s, N-CH_3), 3.88 (2H, br. s, piperidine-CH_2), 4.05 (2H, q, *J* = 7.1 Hz, CH_2-CH_3), 4.23 (2H, br. s, piperidine-CH_2), 4.71 (1H, d, *J* = 12.5 Hz, CH_2-S), 4.86 (1H, d, *J* = 12.5 Hz, CH_2-S), 5.16 (1H, d, *J* = 3.8 Hz,

pyrimidine-CH), 7.20-7.26 (2H, m, Ar-H), 7.27-7.29 (1H, m, Ar-H), 7.31-7.37 (2H, m, Ar-H), 8.09 (1H, d, *J* = 3.8 Hz, NH). ^{13}C-NMR (100 MHz, DMSO): 14.0, 23.7, 24.7, 29.6, 35.6, 50.9, 52.5, 60.2, 106.1, 126.2, 127.7, 129.0, 143.3, 146.4, 153.1, 165.0, 193.7. EI-MS: m/z (%): 433 (M^+, 17). Anal. Calcd. for $C_{21}H_{27}N_3O_3S_2$ (433.15): C, 58.17; H, 6.28; N, 9.69. Found: C, 58.13; H, 6.26; N, 9.71.

*4.1.6.3. Ethyl 6-((dicyclohexylcarbamothioylthio)methyl)-1-methyl-2-oxo-4-phenyl-1,2,3,4-tetrahydropyrimidine-5-carboxylate (**19**)*

Yield (0.38 g, 48 % yield) as off-white solid with m.p. 107–108 °C. IR (KBr) (υ, cm^{-1}): 862 (C-S str.), 1084 (C=S str.), 1523 (C=C str.), 1642 (C=O amide), 1728 (C=O ester), 3010 (C-H Ar. str.), 3250 (NH). ^{1}H-NMR (400 MHz, DMSO): 1.02-1.22 (4H, m, cyclohexyl-CH_2), 1.11 (3H, t, *J* = 7.0 Hz, CH_3-CH_2), 1.25-1.43 (6H, br. s, cyclohexyl-CH_2), 1.48-1.65 (4H, m, cyclohexyl-CH_2), 1.65-1.90 (6H, m, cyclohexyl-CH_2), 3.11 (3H, s, N-CH_3), 3.16 (2H, m, cyclohexyl-CH), 4.04 (2H, q, *J* = 7.0 Hz, CH_2-CH_3), 4.61 (1H, s, CH_2-S), 4.84 (1H, s, CH_2-S), 5.14 (1H, d, *J* = 3.2 Hz, pyrimidine-CH), 7.25 (3H, dd, *J* = 14.0, 7.0 Hz, Ar-H), 7.32 (2H, t, *J* = 7.0 Hz Ar-H), 8.10 (1H, d, *J* = 3.2 Hz, NH). ^{13}C-NMR (100 MHz, DMSO): 13.9, 24.7, 25.7, 29.6, 30.6, 35.9, 52.3, 58.9, 60.2, 106.1, 126.2, 127.6, 128.6, 143.3, 146.8, 152.9, 164.8, 193.8. EI-MS: m/z (%): 529 (M^+, 77). Anal. Calcd. for $C_{28}H_{39}N_3O_3S_2$ (529.24): C, 63.48; H, 7.42; N, 7.93. Found: C, 63.50; H, 7.43; N, 7.94.

*4.1.6.4. Ethyl 1-methyl-2-oxo-4-phenyl-6-((4-phenylpiperazine-1-carbonothioylthio)methyl)-1,2,3,4-tetrahydropyrimidine-5-carboxylate (**20**)*

Yield (0.34 g, 45%) as off-white solid with m.p. 104–105 °C. ^{1}H-NMR (500 MHz, $CDCl_3$): 1.18 (3H, t, *J* = 7.1 Hz, CH_3-CH_2), 3.30 (3H, s, N-CH_3), 3.32-3.47 (4H, m, piperazine-2CH_2), 3.55-3.64 (4H, m, piperazine-2CH_2), 4.12 (2H, q, *J* = 7.1 Hz, CH_2-CH_3), 4.73 (1H, s, CH_2-S), 4.88 (1H, s, CH_2-S), 5.36 (1H, s, pyrimidine-CH), 5.41 (1H, s, NH), 7.22 (1H, m, Ar-H), 7.26-7.40 (4H, m, Ar-H), 7.46 (1H, m, Ar-H), 7.49-7.53 (2H, m, Ar-H), 7.61-7.83 (2H, m, Ar-H). ^{13}C-NMR (125 MHz, DMSO): 13.9, 29.6, 35.7, 49.6, 50.2, 52.5, 60.2, 106.1, 114.3, 121.8, 126.1, 127.6, 128.5, 129.0, 136.6, 143.3, 146.3, 152.9, 164.8, 193.4. EI-MS: m/z (%): 510 (M^+, 91). Anal. Calcd. for $C_{26}H_{30}N_4O_3S_2$ (510.18): C, 61.15; H, 5.92; N, 10.97. Found: C, 61.13; H, 5.95; N, 11.00.

*4.1.6.5. Ethyl 6-((4-(2-ethoxyphenyl)piperazine-1-carbonothioylthio)methyl)-1-methyl-2-oxo-4-phenyl-1,2,3,4-tetrahydropyrimidine-5-carboxylate (**21**)*

Yield (0.39 g, 47%) as white solid with m.p. 110–111 °C. IR (KBr) (υ, cm^{-1}): 857 (C-S str.), 1078 (C=S str.), 1516 (C=C str.), 1635 (C=O amide), 1724 (C=O ester), 2983 (C-H Ar. str.), 3266 (NH). ^{1}H-NMR (500 MHz, $CDCl_3$): 1.18 (3H, t, *J* = 7.1 Hz, CH_3-CH_2), 1.47 (3H, t, *J* = 6.9 Hz, CH_3-CH_2), 2.59-2.63 (4H, m, piperazine-CH_2), 3.29 (3H, s, N-CH_3), 3.31-3.47 (2H, m, piperazine-CH_2), 3.82 (2H, m, piperazine-CH_2), 4.11 (2H, q, *J* = 7.1 Hz, CH_2-CH_3), 4.16 (2H, q, *J* = 6.9 Hz, CH_2-CH_3), 4.89 (1H, s, CH_2-S), 4.96 (1H, s, CH_2-S), 5.37 (1H, d, *J* = 3.1 Hz, pyrimidine-CH), 5.42 (1H, d, *J* = 3.1 Hz, NH), 6.98-7.07 (3H, m, Ar-H), 7.23 (1H, d, *J* = 1.5 Hz, Ar-H), 7.26-7.34 (4H, m, Ar-H), 7.40 (1H, t, *J* = 7.7 Hz, Ar-H). ^{13}C-NMR (125 MHz, DMSO): 13.9, 14.8, 29.6, 35.7, 49.5, 50.1, 52.5, 60.2, 63.4, 106.1, 113.0, 118.4, 120.9, 123.0, 126.2, 127.6, 128.7, 140.1, 143.3, 146.3, 151.2, 152.9, 164.7, 193.4. EI-MS: m/z (%): 554 (M^+, 62). Anal. Calcd. for $C_{28}H_{34}N_4O_4S_2$ (554.20): C, 60.62; H, 6.18; N, 10.10. Found: C, 60.65; H, 6.21; N, 10.11.

*4.1.6.6. Ethyl 6-((4-(4-methoxyphenyl)piperazine-1-carbonothioylthio)methyl)-1-methyl-2-oxo-4-phenyl-1,2,3,4-tetrahydropyrimidine-5-carboxylate (**22**)*

Yield (0.34 g, 42%) as white solid with m.p. 105–106 °C. ^{1}H-NMR (400 MHz, DMSO): 1.12 (3H, t, *J* = 7.1 Hz, CH_3-CH_2), 3.14 (3H, s, N-CH_3), 3.15 (4H, m, piperazine-CH_2), 3.69 (3H, s, O-CH_3), 4.05 (4H,

m, piperazine-CH_2), 5.18 (1H, s, pyrimidine-CH), 6.85 (2H, d, *J* = 8.1 Hz, Ar-H), 6.93 (2H, d, *J* = 8.1 Hz, Ar-H), 7.24-7.26 (3H, m, Ar-H), 7.29-7.34 (2H, m, Ar-H), 8.12 (1H, s, NH). ^{13}C-NMR (100 MHz, DMSO): 13.9, 29.6, 35.7, 49.6, 50.0, 52.5, 56.0, 60.2, 106.1, 115.1, 115.2, 126.2, 127.6, 128.6, 137.4, 143.3, 146.3, 152.8, 153.0, 164.7, 193.5. EI-MS: m/z (%): 540 (M^+, 33). Anal. Calcd. for $C_{27}H_{32}N_4O_4S_2$ (540.19): C, 59.98; H, 5.97; N, 10.36. Found: C, 59.99; H, 6.01; N, 10.37.

4.2. Biology

4.2.1. Preliminary in vitro anticancer screening

In vitro cytotoxicity of compounds **6**, **7**, **9**-**12**, **15**, **17**–**20** and **22** was evaluated according to the current one-dose protocol of the National Cancer Institute (NCI, USA) assay against a panel of 60 tumor cell lines at 10 μM concentration [37].

4.2.2. MTT assay for cytotoxicity

In vitro cytotoxicity (IC_{50}) of compounds **13**, **14**, **16** and **21** was tested by using a standard colorimetric method (MTT assay) against three human tumor cell lines including human prostate cancer (PC-3), colorectal carcinoma (HCT-116) and breast cancer (MCF-7) obtained from ATCC *via* Holding company for biological products and vaccines (VACSERA), Cairo, Egypt. Cell lines were cultured in RPMI-1640 medium with 10% fetal bovine serum. Penicillin and streptomycin were added at 37 °C. Cells were seed in a 96-well plate at 37 °C for 48 h. After incubation the cells were treated with different concentration of compounds and incubated for 24 h. After 24 h of drug treatment, 20 μL of MTT solution at 5 mg/mL was added and incubated for 4 h. 100 μL of Dimethyl sulfoxide (DMSO) was added into each well to dissolve the purple formazan formed. The colorimetric assay is measured and recorded at absorbance of 570 nm using a plate reader (EXL 800, USA). The relative cell viability in percentage was calculated as (A570 of treated samples/A570 of untreated sample) x 100 [38].

4.2.3. Enzyme-Linked Immunosorbent Assay of caspase-3 and caspase-9

4.2.3.1. The Invitrogen Caspase-3 (active) Human ELISA assay

The number of 8-well strips needed for the assay was determined. The standard diluent buffer (100 μL) was added to the zero standard wells, while chromogen blank was left empty. The standards, controls and tested compound (100 μL) were then added, and incubated for 2 hours at room temperature. Wells were evacuated from liquids, and washed 4 times. Caspase-3 (active) detection antibody solution (100 μL) was added to each well except the chromogen blank(s), and incubated for 1 hour at room temperature. Again liquid was discarded from wells and washed 4 times. Anti-Rabbit IgG HRP working solution was then added to each well except the chromogen blank and incubated for 30 minutes at room temperature. Wells were washed 4 times. Stabilized Chromogen (100 μL) was added to each well, and incubated for 30 minutes at room temperature. Finally, stop solution (100 μL) was added to each well and the absorbance was read at 450 nm within 2 hours after addition. Curve fitting software was used to generate the standard curve; from which the concentrations for tested compound and controls were read.

4.2.3.2. DRG® Caspase-9 (human) ELISA (EIA-4860) assay

First, cell lysates were prepared. The number of required microwell strips was determined and allowed to be washed twice with wash buffer. The sample diluent was added in duplicate to the blank wells (100 μL) and to sample wells (50 μL). The sample was added in duplicate (50 μL) to designated sample wells. Detection antibody (50 μL) was prepared and added to all wells, and incubated for 2 hours at room temperature. Microwell strips were washed 3 times with wash buffer. Anti-rabbit-IgG-HRP was

prepared and added (100 µL) to all wells, then incubated for 1 hour at room temperature. Microwell strips were washed 3 times with wash buffer. TMB substrate solution (100 µL) was added, and incubated for 10 minutes at room temperature. Finally, stop solution (100 µL) was added, and the color intensity was measured at 450 nm.

4.2.4. Cell cycle analysis and induction of apoptosis

4.2.4.1. Flow cytometric analysis of cell-cycle distribution

For flow cytometric analysis of DNA content, A549 cells in exponential growth were treated with compound **19** and incubated for 24 h. The cells were collected, centrifuged and fixed with ice cold ethanol (70%). The cells were then treated with buffer containing RNAse A and 0.1% Triton X-100, then stained with propidum iodide (PI) and compared with control which was treated with DMSO. DNA contents were measured by flow cytometry.

4.2.4.2. Analysis of cellular apoptosis

A549 cells in exponential growth were treated with compounds **19** and incubated for 24 h. After an incubation period, 1-5 x 10^5 cells were harvested and suspended in 500 µL of 1X Binding Buffer, 5 µL of Annexin V-FITC and 5 µL of PI. They are incubated at room temperature for 5 min in the dark and incubated at 37 °C. Annexin V-FITC conjugate is specially engineered to produce enhanced fluorescence signal and photo stability. The Annexin V-FITC kit includes Annexin V-FITC for detecting apoptosis and PI for detecting necrosis. Thus, Apoptosis and necrosis can be differentiated. Detection and analyzing of Annexin V-FITC binding by flow cytometry (Ex = 488 nm; Em = 530 nm) using FITC signal detector (usually FL1) and PI staining by the phycoerythrin emission signal detector (usually FL2). Visit *http://www.biovision.com* for details.

4.2.5. Enzyme activity inhibition assay

4.2.5.1. VEGFR-2 inhibition assay

The enzyme inhibition assay of compounds **14** and **19** against VEGFR-2 was evaluated using the RayBio® Human VEGFR-2 ELISA (Enzyme-Linked Immunosorbent Assay) kit. The assay utilized a specific antibody for human VEGFR-2 coated on a 96-well plate, where 100 µL of either standard solution or tested compound was added to each well and incubated for 2.5 hours at room temperature. Wells were washed; prepared biotin antibody (100 µL) was added and incubated for 1 hour at room temperature. The unbound biotinylated antibody was washed away from each well; prepared Streptavidin solution (100 µL) was added and incubated for 45 minutes at room temperature. Wells were washed again followed by addition of TMB One-Step Substrate Reagent (100 µL) to each well and incubated for 30 minutes at room temperature, where the color was produced proportionally to the amount of bound VEGFR-2. Stop solution (50 µL) was added to each well and the color intensity was read at 450 nm immediately. The mean absorbance for each set of duplicate standards controls and tested compounds was calculated, and the average zero standard optical density was subtracted. The standard curve was plotted on log-log graph paper with standard concentration on the X-axis and absorbance on the Y-axis. % Inhibition was calculated *via* comparing results obtained from test compounds with control, while IC_{50} was calculated from concentration/inhibition response curve compared to sorafenib as a standard. Visit *http://www.raybiotech.com* for details.

4.2.5.2. mTor inhibition assay

The enzyme inhibition assay of compounds **14** and **19** against mTOR was evaluated using Abcam's mTOR *in vitro* SimpleStep ELISA® (Enzyme-Linked Immunosorbent Assay) kit. This assay employs an affinity tag labeled capture antibody and a reporter conjugated detector antibody which immunocapture the sample analyte in solution. This entire complex (capture antibody/analyte/detector antibody) is in turn immobilized *via* immunoaffinity of an anti-tag antibody coating the well.
To perform the assay, tested compounds or standards (50 µL) were added to the 96 well plate strips included with the kit, followed by the antibody mix (50 µL). All standards, controls and tested compounds were assayed in duplicates. After incubation for 1 hour at room temperature, the wells were washed with 3 x 350 µL 1X Wash Buffer PT to remove unbound material. TMB substrate (100 µL) was added, incubated for 10 minutes in the dark, and then catalyzed by HRP, generating blue coloration. This reaction was then stopped by addition of Stop Solution (100 µL), shaken on a plate shaker for 1 minute to mix and complete any color change from blue to yellow. Signal was generated proportionally to the amount of bound analyte and the intensity is measured at 450 nm. % Inhibition was calculated *via* comparing results obtained from test compounds with control, while IC_{50} was calculated from concentration/inhibition response curve compared to rapamycin as a standard. Visit *http://www.abcam.com* for details.

5. Acknowledgment

We thank Dr. M. Youssif for his help during proofreading the article and Dr. George S. G. Shehatou for his assistance in revision of biology section.

6. References

[1] Nelson, D.L., Lehninger A.L., Cox M.M. Lehninger principles of biochemistry. 5th Ed. New York (NY), 2008: W. H. Freeman.
[2] Radha, V., Nambirajan, S., Swarup, G. Association of Lyn tyrosine kinase with the nuclear matrix and cell-cycle-dependent changes in matrix-associated tyrosine kinase activity. Eur. J. Biochem. 236 (1996) 352–359.
[3] Senger, D.R., Galli, S.J., Dvorak, A.M., et al. Tumor cells secrete a vascular permeability factor that romotes accumulation of ascites fluid. Science 219 (1983) 983–985.
[4] Carmeliet, P., Jain, R.K. Molecular mechanisms and clinical applications of angiogenesis. Nature 473 (2011) 298–307.
[5] Ou, J.M., Yu, Z.Y., Qiu, M.K., Dai, Y.X., Dong, Q., Shen, J., Dong, P., Wang, X.F., Liu, Y.B., Quan, Z.W., Fei, Z.W. Knockdown of VEGFR2 inhibits proliferation and induces apoptosis in Hemangioma-derived endothelial cells. Eur. J. Histochem. 58 (2014) 2263–2270.
[6] Liang, Y., Brekken, R. A., Hyder, S.M. Vascular endothelial growth factor induces proliferation of breast cancer cells and inhibits the anti-proliferative activity of anti-hormones. Endocr. Relat. Cancer 13(2006) 905–919.
[7] Paesler, J., Gehrke, I., Poll-Wolbeck, S.J., Kreuzer, K.A. Targeting the vascular endothelial growth factor in hematologic malignancies. Eur. J. Haematol. 89(2012) 373–384.
[8] Sabbah, D.A., Brattain, M.G., Zhong, H. Dual inhibitors of PI3K/mTOR or mTOR-selective inhibitors: Which way shall we go? Curr. Med. Chem. 18 (2011) 5528–5544.
[9] Zheng, Y., Jiang, Y. mTOR inhibitors at a Glance. Mol. Cell Pharmacol. 7 (2015) 15–20.
[10] Rodon, J., Dienstmann, R., Serra, V., Tabernero, J. Development of PI3K inhibitors: lessons learned from early clinical trials. Nat. Rev. Clin. Oncol. 10 (2013) 143–153.
[11] Markman, B., Tao, J.J., Scaltriti, M. PI3K pathway inhibitors: better not left alone. Curr. Pharm. Des. 19 (2013) 895–906.
[12] Manara, M. C., Nicocetti, G., Zambelli, D., Ventura. S., Guerzoni, C., Landuzzi, L., Lollini, P., Maira, S., García-Echeverría, C., Mercuri, M., Picci, P., Scotlandi, K. NVP-BEZ235 as a New Therapeutic Option for Sarcomas Clin. Cancer Res. 16 (2010) 530–540.
[13] Biginelli, P. Aldehyde-urea derivatives of aceto- and oxaloacetic acids. Gazz. Chim. Ital. 23 (1893) 360–413.
[14] Kaur, R., Chaudhary, S., Kumar, K., Gupta, M.K., Rawal, R.K. Recent synthetic and medicinal perspectives of dihydropyrimidinones: A review. Eur. J. Med. Chem. 132 (2017) 108–134.

[15] Ashok, M., Holla, B., Kumari, N. Convenient one pot synthesis of some novel derivatives of thiazolo[2,3-b] dihydropyrimidinone possessing 4- methylthiophenyl moiety and evaluation of their antibacterial and antifungal activities. Eur. J. Med. Chem. 42 (2007) 380–385.
[16] Naidu, B.N., Sorenson, M.E., Patel, M., Ueda, Y., Banville, J., Beaulieu, F., Bollini, S., Dicker, I.B., Higley, H., Lin, Z. Synthesis and evaluation of C2-carbon-linked heterocyclic-5-hydroxy-6-oxo-dihydropyrimidine-4-carboxamides as HIV-1 integrase inhibitors. Bioorg. Med. Chem. Lett. 25 (2015) 717–720.
[17] de Vasconcelos, A., Oliveira, P.S., Ritter, M., Freitag, A., Romano, L., Quina, F.H., Pizzuti, L., Pereira, C.M.P., Francieli, M. Antioxidant capacity and environmentally friendly synthesis of dihydropyrimidin-(2H)-ones promoted by naturally occurring organic acids. J. Biochem. Mol. Toxicol. 26 (2012) 155–161.
[18] Stefani, H.A., Oliveira, C.B., Almeida, R.B., Pereira, C.M.P., Braga, R.C., Cella, R., Borges, V.C., Savegnago, L., Nogueira, C.W. Dihydropyrimidin-(2H)-ones obtained by ultrasound irradiation: a new class of potential antioxidant agents. Eur. J. Med. Chem. 41 (2006) 513–518.
[19] Mayer, T.U., Kapoor, T.M., Haggarty, S.J., King, R.W., Schreiber, S.I., Mitchison, T.J. Small molecule inhibitor of mitotic spindle bipolarity identified in a phenotype-based screen. Science 268 (1999) 971–974.
[20] Russowsky, D., Canto, R.F.S., Sanches, S.A.A., D'Oca, M.G.M., de Fátima, Â., Pilli, R.A., Kohn, L.K., Antônio, M.A., de Carvalho, J.E. Synthesis and differential antiproliferative activity of Biginelli compounds against cancer cell lines: Monastrol, oxo-monastrol and oxygenated analogues. Bioorg. Chem. 34 (2006) 173–182.
[21] Gartner, M., Sunder-Plassmann, N., Seiler, J., Utz, M., Vernos, I., Surrey, T., Giannis, A. Development and biological evaluation of potent and specific inhibitors of mitotic Kinesin Eg5. ChemBioChem. 6 (2005) 1173–1177.
[22] Kaur, N., Kaur, K., Raj, T., Kaur, G., Singh, A., Aree, T., Park, S-J., Kim, T-J., Singh, N., Jang, D.O. One-pot synthesis of tricyclic dihydropyrimidine derivatives and their biological evaluation. Tetrahedron 71 (2015) 332–337.
[23] Ragab, F.A.F., Abou-Seri, S.M., Abdel-Aziz, S.A., Alfayomy, A.M., Aboelmagd, M. Design, synthesis and anticancer activity of new monastrol analogues bearing 1,3,4-oxadiazole moiety. Eur. J. Med. Chem. 138 (2017) 140–151.
[24] Wright, C.M., Chovatiya, R.J., Jameson, N.E., Turner, D.M., Zhu, G., Werner, S., et al. Pyrimidinone-peptoid hybrid molecules with distinct effects on molecular chaperone function and cell proliferation. Bioorg. Med. Chem. 16 (2008) 3291–3301.
[25] Martins, P., Jesus, J., Santos, S., Raposo, L.R., Roma-Rodrigues, C., Baptista, P.V., Fernandes, A.R. Heterocyclic anticancer compounds: Recent advances and the paradigm shift towards the use of nanomedicine's tool box. Molecules 20 (2015) 16852–16891.
[26] Akhtar, J., Khan, A.A., Ali, Z., Haider, R., Yar, M.S. Structure-activity relationship (SAR) study and design strategies of nitrogen-containing heterocyclic moieties for their anticancer activities. Eur. J. Med. Chem. 125 (2017) 143−189.
[27] Zheng, Y., Duan, Y., Ma, J., Xu, R., Zi, X., Lv, W., Wang, M., Ye, X., Zhu, S., Mobley, D. et al. Triazole−dithiocarbamate based selective lysine specific demethylase 1 (LSD1) inactivators inhibit gastric cancer cell growth, invasion, and migration. J. Med. Chem. 56 (2013) 8543−8560.
[28] Besoluk, S., Kucukislamoglu, M., Nebioglu, M., Zengin, M., Arslan, M. Solvent-free synthesis of dihydropyrimidinones catalyzed by alumina sulfuric acid at room temperature. J. Iran. Chem. Soc. 5 (2008) 62–66.
[29] Zigeuner, G., Hamberger, H., Blaschke, H., Sterk, H. Über Heterocyclen, 12. Mitt.: Zur Bromierung der 2-Oxo-6-methyltetrahydropynimidine. Monatsh. Chem. 97 (1966) 1408–1421.
[30] Kappe, C.O. Unexpected Formation of Nitriles from Reactions of 6-(Dibromomethy1)-1,2,3,4-tetrahydro-2-oxo-5-pyrimidinecarboxylates with sodium azide. Liebigs Ann. Chem. (1990) 505–507.
[31] Khanetskyy, B., Dallinger, D., Kappe, C.O. Combining Biginelli multicomponent and click chemistry: Generation of 6-(1,2,3-triazol-1-yl)-dihydropyrimidone libraries. J. Comb. Chem. 6 (2004) 884–892.
[32] Kolb, H.C., Finn, M.G., Sharpless, K.B. Click chemistry: Diverse chemical function from a few good reactions. Angew. Chem. Int. Ed. 40 (2001) 2004–2021.
[33] Rostovtsev, V.V., Green, L.G., Fokin, V.V., Sharpless, K.B. A stepwise Huisgen cycloaddition process: Copper(I)-catalyzed regioselective "ligation" of azides and terminal alkynes. Angew. Chem. Int. Ed. 41 (2002) 2596–2599.
[34] Andersson, M., Sjöstrand, J., Petersen, A., Honarvar, A.K., Karlsson, J.O. Caspase and proteosome activity during staurosporin-induced apoptosis in lens epithelial cells. Invest. Optthalmol. Vis. Sci. 41 (2000) 2623–2632.
[35] Boatright, K.M., Salvesen, G.S. Mechanisms of caspase activation. Curr. Opin. Cell Biol. 15 (2003) 725–731.
[36] Daina, A., Michielin, O., Zoete, V. SwissADME: a free web tool to evaluate pharmacokinetics, drug-likeness and medicinal chemistry friendliness of small molecules. *Sci. Rep.* (2017) 7:42717.
[37] Skehan, P., Storeng, R., Scudiero, D., Monks, A., McMahon, J., Vistica, D., Warren, J.T., Bokesch, H., Kenney, S., Boyd, M.R. New colorimetric cytotoxicity assay for anticancer-drug screening. J. Natl. Cancer Inst. 82 (1990) 1107–1112.
[38] Mosmann, T. Rapid colorimetric assay for cellular growth and survival application to proliferation and cytoyoxic assays. J. Immunol. Methods 65 (1983) 55–63.

Highlights

- A new series of dihydropyrimidinones was designed and synthesized.
- Cytotoxic activity was assessed against 60 cancer cell lines.
- Compound **19** showed a significant activity against NCI-H460, SK-MEL-5, and HL-60(TB) cell lines.
- Compound **19** induced apoptosis and showed cell cycle arrest at G2/M phase.
- Compounds **14** and **19** showed lower cytotoxic activity than doxorubicin against three normal cells.
- Compound **19** exhibited a 1.5-fold increase in mTOR enzyme activity over that of rapamycin.

Highlights

- A new series of dihydropyrimidinones was designed and synthesized.
- Cytotoxic activity was assessed against 60 cancer cell lines.
- Compound **19** showed a significant activity against NCI-H460, SK-MEL-5, and HL-60(TB) cell lines.
- Compound **19** induced apoptosis and showed cell cycle arrest at G2/M phase.
- Compounds **14** and **19** showed lower cytotoxic activity than doxorubicin against three normal cells.
- Compound **19** exhibited a 1.5-fold increase in mTOR enzyme activity over that of rapamycin.